Effects of H2 addition on combustion and exhaust emissions in a diesel engine- Using a 3D Model with Chemical Kinetics

Hassan A. Khairallah

Department of Mechanical Engineering, Tobruk University , Tobruk, Libya

Abstract

During the past decade, considerable efforts have been made to introduce alternative fuels for use in conventional diesel and gasoline engines. There is significant interest in adding hydrogen to a diesel engine to reduce emissions and improve efficiency. With the rapid increase in computational capabilities, computational fluid dynamics (CFD) codes have become essential tools for the design, control, and optimization of dual fuel engines. In the present study, a reduced chemical kinetics mechanism, consisting of 52 reactions and 29 chemical species for n-heptane fuel combustion, was incorporated with detailed chemical kinetics consisting of 29 reactions for hydrogen including additional nitrogen oxidation. This reaction mechanism was coupled with a 3D CFD model based on AVL FIRE software to investigate the performance and emission characteristics of a diesel engine with low amounts of hydrogen addition. The hydrogen was substituted for diesel fuel with verity levels (4.83 %, 6.43 % and 11.6 % by volume). The injection timing of the pilot diesel was constant at 23 BTDC, and the injection duration is adjusted to 30 crank angle degrees.The model was validated by the experimental results and then employed to examine important parameters that have significant effects on the engine performance. The simulation results showed that the variations of CO_2, CO and NO_X emissions reasonably agree with the experimental findings. NO_X emissions and exhaust gas temperature increased with the rise in brake power for hydrogen-diesel mixtures. The CFD results quantified the degree of dependence of NO_X emissions on the average combustion temperature. The results also quantified that CO and CO_2 emissions decreased when adding hydrogen in diesel engine because the addition of hydrogen leads to reduction in the injected amount of diesel fuel that results in CO and CO_2 formation.

Keywords: detailed chemical kinetics , AVL FIRE®, diesel engine, hydrogen , emissions.NOx formation.

I. INTRODUCTION

Due to the depletion of fossil fuels and environmental degradation in recent years, there is considerable global effort to ensure continued availability of supplies of hydrocarbon fuels and to reduce exhaust emissions from all combustion devices, particularly internal combustion engines. Many studies by a number of research groups worldwide have focused attention on alternative transportation fuels to replace or supplement hydrocarbon fuels.In this regard, hydrogen is considered one of the most promising alternate fuels due to its clean burning characteristics and better overall performance as compared to diesel. Some of the important properties of hydrogen are given in Table 1 [1-2]. Hydrogen has a wide flammability range in comparison with all other fuels. As a result, hydrogen can be used in running an engine on a lean mixture that allows for greater fuel economy due to a more complete combustion of the fuel. Additionally, it allows for lower combustion temperature and hence decreases the amount of NOx. The ignition energy required to ignite the hydrogen is also very low, which allows hydrogen engine to ignite lean mixtures and ensures prompt ignition even with a relatively weak spark. However, hydrogen cannot be used directly in a diesel engine because it is very difficult to ignite it by only the compression process due to its auto-ignition temperature (858 K) being so much higher than that of diesel fuel (525 K) [3]. Therefore, some of the auxiliary ignition sources (spark plugs, glow plugs, or pilot fuel) [3, 4, 5, 6, 7,] have to be used inside the combustion chamber to ensure the ignition of hydrogen. In this work, hydrogen was used as a supplemental fuel in a diesel engine to replace a portion of the diesel fuel burned in the engine. Diesel fuel, with its low auto-ignition temperature can be used as a pilot fuel to ignite hydrogen.

Table 1 Properties of hydrogen in comparison with diesel

Properties	Hydrogen	Diesel
Auto-ignition temperature (K)	858	530
Minimum ignition energy (mJ)	0.02	-
Flammability limits in air (vol. %)	4-75	-
Net heating value (MJ/kg)	119.9	42.2
Stoichiometric air/fuel (mass)	34.3	14.5
Density at ambient temperature (kg/m^3) @ 1.01 bar	0.083	824
Quenching gap in NTP air (cm)	0.064	-
Stoichiometric flame speed (m/s)	2.65-3.25	0.3

Computational fluid dynamics (CFD) has considered a powerful numerical tool to simulation of many processes in industry.It provides deeper understanding of what is happening inside the combustion cylinder.Consequently it will give the ability to predict the performance of new designs with much less time and costs compered to experimental investigation.

In the present work, a reduced reaction mechanism consisting of 52 reaction steps with 29 chemical species for n-Heptane fuel combustion was incorporated with detailed chemical kinetic reactions consisting of 29 reaction steps for hydrogen, including additional nitrogen oxidation reactions. This reaction mechanism was coupled with the AVL FIRE® CFD code to compare the performance and emission characteristics of a DI diesel engine with hydrogen as the fuel mixing with diesel as the source of ignition.

An advantage of this model is the FIRE General Gas Phase Reactions Module was used for simulation of dual fuel engine that run on either diesel/hydrogen mixture or diesel with others conventional fuels (methane or gasoline), contrary to what it is done in most existing engines models.

Computational Methods

AVL FIRE® presents a general species transport model to allow the implementation of a detailed kinetic model [8] andsolves species transport equations for any arbitrary number of chemical species. The species mass conservation equation is expressed as

$$\frac{\partial(\rho w_i)}{\partial t} + \frac{\partial}{\partial x_k}(\rho(U_k - U_{\delta k})w_i)$$
$$= \frac{\partial}{\partial x_k}\left(\left(\rho D_i + \frac{\mu}{\sigma_{ci}}\right)\frac{\partial}{\partial x_k}\right) + S_{w_i} \qquad (1)$$

$$S_{w_i} = r_i$$

Where w_i is the mass fraction, S_{w_i} is the source term of species i by taking into account homogeneous chemical reactions, σ_{ci} is the stress tensor, and μ is the viscosity. The thermophysical properties (viscosity, density, specific heat, diffusion coefficient, thermal conductivity) shown in the equation above are calculated for each species and for gas mixtures by using the chemical kinetic databases (CHEMKIN™).

The chemistry effect (level of elementary reactions) is taken into account such that at the beginning of each CFD time step (Δt), a single zone reactor model is calculated for each computational cell. At the latest CFD time step for the properties (pressure, volume, temperature), the following conservation equations are integrated by the model for the time step (Δt), considering the volume cell as a function of time. The species conservation equation is computed using:

$$\rho \frac{\partial w_i}{\partial t} = M_i \omega_i \tag{2}$$

where M_i is the molecular weight of ith species, and ω_i is the molar production rate of species. In this case, only the source term, S_{w_i}, is taken into account due to the homogeneity assumption. The energy conservation equation is expressed as:

$$\rho c_v \frac{\partial T}{\partial t} + \frac{P}{V} \frac{\partial V}{\partial t} = -\sum_{i=1}^{N_y} u_i M_i \omega_i \tag{3}$$

On the left-hand side, the first term represents the temporal change of energy content, and the second term represents the volume work. The terms on the right-hand side represent the consideration of the change of inner energy due to production and consumption of chemical species. By using an interface to the CHEMKIN™ libraries, the molar species production rates, ω_i, can be calculated, and the source terms can be calculated by neglecting any effect of turbulence/mixing on the chemical reaction as follows:

$$r_i = \frac{\rho^{n+1} w_i^{n+1} - \rho^n w_i^n}{\Delta t} \tag{4}$$

where the superscripts n and n+1 indicate the first and the last values of the single zone reactor model. Keeping the source terms constant for the following CFD time step is the most important advantage of this approach because it makes the CFD simulation 100 percent conservative, fast, and valid.

The following approach considers the effects of both mixing and chemical kinetics by assuming that the reaction rate is determined via a kinetic time scale τ_{kin} (an equilibrium assumption under perfect mixed conditions) and turbulent time scale τ_{turb} (an eddy break up assumption). Furthermore, it assumes that the equilibrium concentration of the fuel is zero and the kinetic time scale is equal to the scale used for the fuel for all species. The time scale of CO is used as a rate-limiting kinetic time step if the fuel concentration approaches zero. By taking these assumptions into account, the above equation becomes

$$r_i = \frac{\tau_{kin}}{\tau_{kin} + f\tau_{turb}} \frac{\rho^{n+1} w_i^{n+1} - \rho^n w_i^n}{\Delta t} \tag{5}$$

$$\tau_{kin,i} = \Delta t \frac{\rho^{n+1} w_i^{n+1}}{\rho^{n+1} w_i^{n+1} - \rho^n w_i^n} \tag{6}$$

$$\tau_{kin} = \max(\tau_{kin,f}, \tau_{kin,CO}) \tag{7}$$

The turbulent time scale τ_{turb} can be calculated using the following:

$$\tau_{turb} = C_t \frac{k}{\varepsilon} \tag{8}$$

The variable f is a delay coefficient that is used to simulate the influence of turbulence on combustion after ignition has occurred [9] and can be calculated as:

$$f = \frac{1 - e^{-r}}{0.632} \tag{9}$$

$$r = \frac{w_{CO_2} - w_{H_2O} - w_{CO} - w_{H_2}}{1 - w_{N_2}} \tag{10}$$

A reduced (52 reactions and 29 species) chemical reaction mechanism for n-Heptane was constructed from a comprehensive detailed n-Heptane mechanism (179 species and 1642 reactions) [10]. n-Heptane was chosen in this study because its cetane number (CN~56) is rather close to that of typical diesel fuels (CN~50).

The reduced reaction mechanism consisting of 52 reaction steps with 29 chemical species for n-Heptane fuel combustion was incorporated with detailed chemical kinetic reactions consisting of 29 reactions steps for hydrogen, which includes additional nitrogen oxidation reactions [11]. Figure 1 shows the skeletal chemistry mechanism for multi-fuels (hydrogen/diesel). The multi-chemical reaction mechanism (89 reactions and 32 species) was coupled with a 3D-CFD model based on AVL FIRE® software.
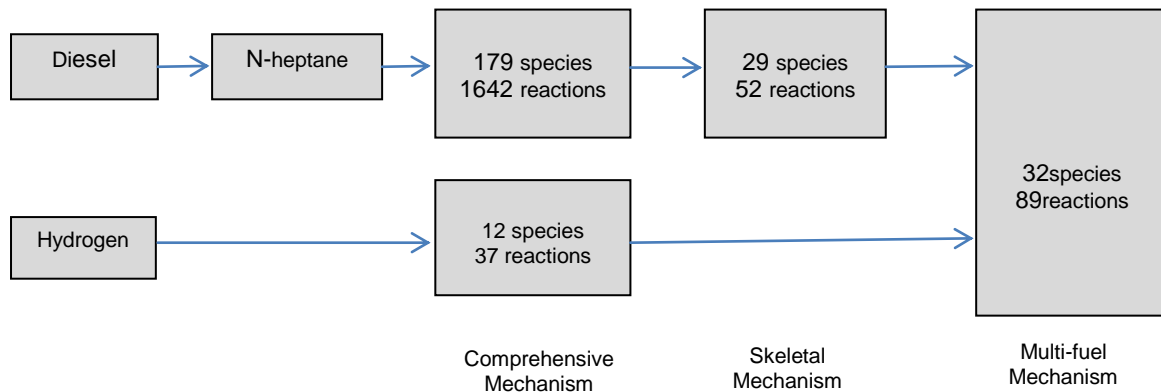

Figure 1 Skeletal chemistry mechanism for multi-fuels.

The CHEMKIN™ chemistry solver was integrated into the AVL FIRE® code for solving the chemistry during multidimensional engine simulation. The AVL FIRE® code provides CHEMKIN™ the species and thermodynamic information of each computation cell, and the CHEMKIN™ utilities return the new species information and energy release after solving for the chemistry.

The piston geometry and computational grid used for the simulations are shown in Figure 2. The mesh was composed of about 7680 computational cells with mesh dimensions of $0.00333 \times 0.00333 \times 0.00356$ m.
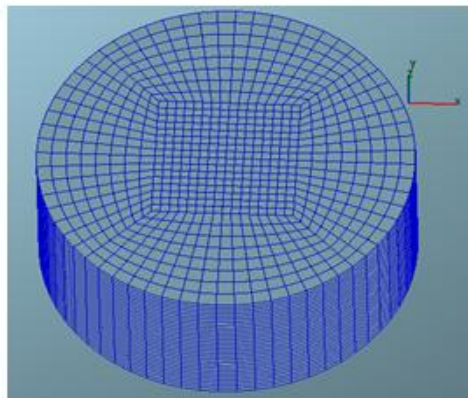

Figure 2 Computational mesh (50 sectors at TDC).
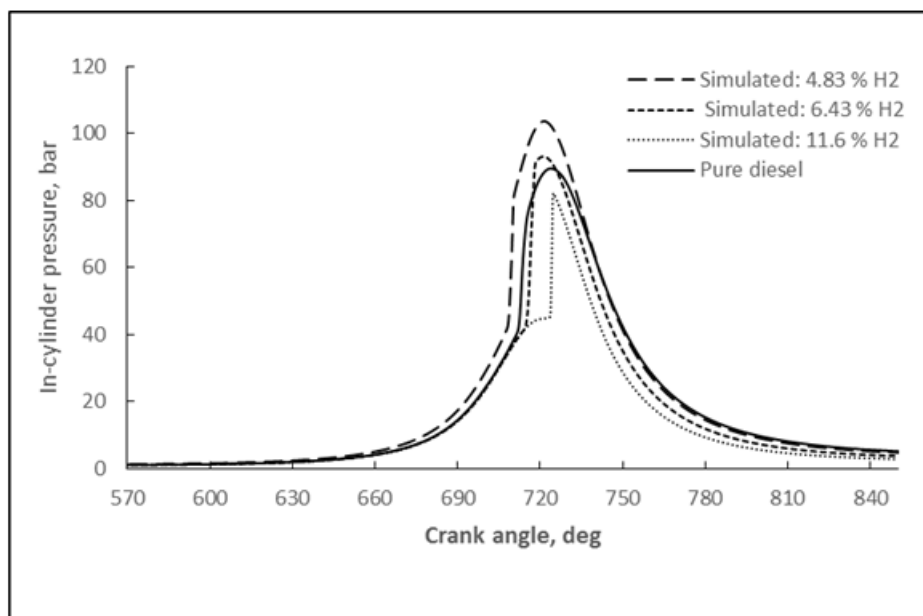
II. RESULTS AND DISCUSSION

In the present work, a multi-chemical reaction mechanism was implemented using 3-D computational fluid dynamics (CFD) based on AVL FIRE® and CHEMKIN™ to investigate the combustion and emission characteristics of a direct ignition (DI) diesel engine with gaseous hydrogen as a fuel and with diesel as the source of ignition. The hydrogen was substituted for diesel fuel with verity levels (4.83 %, 6.43 % and 11.6 % by volume). The injection timing of the pilot diesel (i. e. the crank angle of the start of diesel fuel injection) was constant at 23 BTDC, and the injection duration is adjusted to 30 crank angle degrees. By using theexperiment data, the model were run with same experiment engine condition at each brake power and the results found on good agreement with the experiment results. The operating conditions of the diesel engine modeled and simulated in this investigation were similar to the independent experimental study by Saravanan et al. [8] because their reported test conditions and experimental data were well documented. The specifications of the compression ignition (CI) engine in this computational study are given in Table 2.

Engine Specifications	
No. of cylinders	1
Bore	80 mm
Stroke	110 mm
Speed	1500 rpm
Compression ratio	16.5:1
Type of cooling	Water cooled
Rated output	3.7 kW
Piston type	Flat
No. of injector holes	4
Hole diameter	0.000169 m
spray angle	160º
Operating Conditions	
Fuel amounts by energy %	62.5 % diesel + 37.5 % H2
Initial temperature	333 K
Initial pressure	1 bar
Start of injection	23º BTDC
Duration of injection	30 degree

Pressure

Figure 3 illustrates the variation of cylinder pressure as function with crank angle. Where it can be seen that the peak cylinder pressure for a hydrogen/diesel mixture (4.83 % H2 by volume) was higher (103.7 bar) than that for pure diesel (88.4 bar) for the same operational conditions. This is due to the higher flame speed of hydrogen which will lead to overall faster and more complete combustion, resulting in higher peak pressure.Also the peak pressure occurrence in hydrogen/diesel operation is advanced by 3 crank angles compared to the peak pressure of diesel at full load.This is may be due to that hydrogen undergoes instantaneous combustion compared to diesel.

The figure 4 also illustrates that the peak cylinder pressure decreased gradually with increasing hydrogen level due to lean burn operation (equivalence ratio decreases).
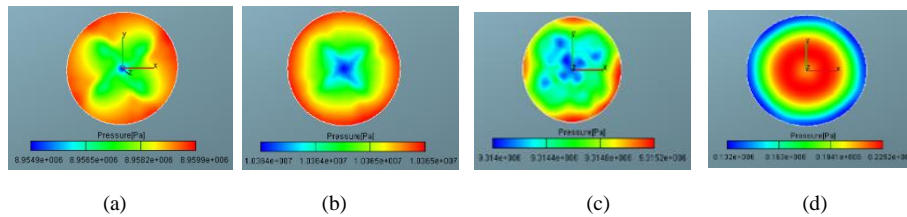
| (a) | (b) | (c) | (d) |

Figure 4. Contour plots for peak pressure at (a) pure diesel (b) 4.83 % H2 (c) 6.43 % H2 (d) 90 % H2

Ignition delay and Combustion Duration

Figure (5) shows ignition delay and combustion duration for various hydrogen level. The ignition delay in diesel engine defined as the time lag between the start of injection to start of the combustion.In the present studythe injection timing of the pilot diesel (i. e. the crank angle of the start of diesel fuel injection) was constant at 23 BTDC. Increasing the hydrogen level led to increase in ignition delay due to a high ignition temperature for hydrogen, and also the amount of diesel fuel to ignite the premixing ofhydrogen with air was reduced and resulted in a late start of combustion. As we can see from figure (5) that the ignition delay with 4.8 % H2 was 10 crank angles while were 8 and 4 crank angles with 9.8 % H2 and 11.8 % H2 respectively. Increasing the hydrogen level reduced the duration of combustion process.This results from the rapid burning of hydrogen. Combustion duration is defined as the interval between the crank angle of the start of combustion and crank angle of the end of combustion. With increasing of H2 dramatically reduced the combustion duration due to hydrogen's high speed of flame propagation.

Crank angle	4.83 % H_2	6.43 % H_2	11.6 % H_2
23BTDC			
14BTDC			
12BTDC			
6BTDC			
4ATDC			
60ATDC			

NO_X emissions

Figure 6 illustrates the predicted and measured NO_X emissions as a function of engine power. It was observed that the NOx emissions increased with the additional brake power for the conditions considered. The NO_X emission with hydrogen/diesel operation was 2700 ppm, which was higher than that of baseline diesel (2089 ppm) at full load. The main reason for the higher concentration of NOx in the hydrogen/diesel operation is the higher combustion temperatures compared to those in the pure diesel operation. The high combustion temperatures can be explained by the high adiabatic flame temperature and the combustion rates of hydrogen [28]. Moreover, the high residence time of the high temperature gases in the cylinder led to the production of higher NOx emissions. The model-predicted trends of NOx emissions are very similar to the experimental results. Also we can see that as the hydrogen level increases, the lean limit of combustion is significantly prolonged, which in turn decreases the peak combustion temperature and hence lead to reduce NO to 490 ppm at 11.6 % H2 by volume with equivalence ratio 0.4.
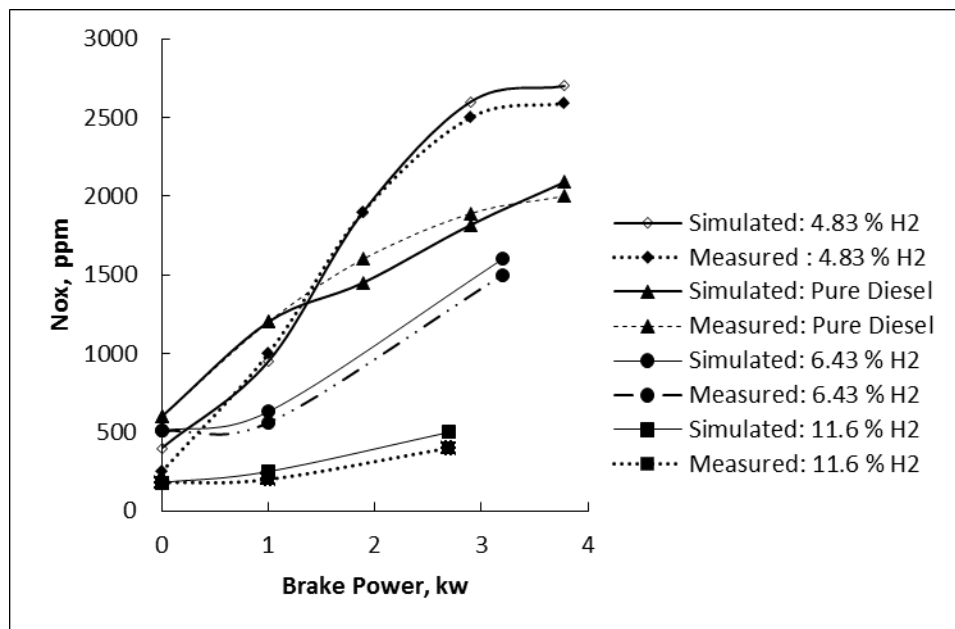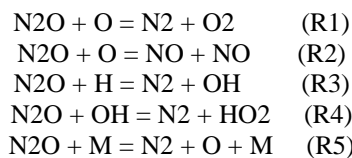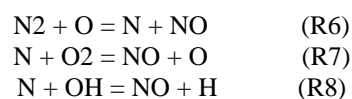

Figure 6Variation of oxides of nitrogen with brake power

As shown in Figure 7, for pure diesel operation, the NO value and the temperature were lower than those for the hydrogen/diesel operation. For both cases, the peak NO value attained the highest value just near TDC (Top Dead Center) in the post-flame region because NO formation is highly temperature dependent. NO is formed mainly as a result of the following reactions:

$$N2O + O = N2 + O2 \qquad (R1)$$
$$N2O + O = NO + NO \qquad (R2)$$
$$N2O + H = N2 + OH \qquad (R3)$$
$$N2O + OH = N2 + HO2 \qquad (R4)$$
$$N2O + M = N2 + O + M \qquad (R5)$$

The other path to NOx formation can be described by reactions R6, R7, and R8, usually known as the extended Zel'dovich mechanism:

$$N2 + O = N + NO \qquad (R6)$$
$$N + O2 = NO + O \qquad (R7)$$
$$N + OH = NO + H \qquad (R8)$$

Normally, these three reactions are only important at high temperatures because radicals O and OH are created in high temperature gases.

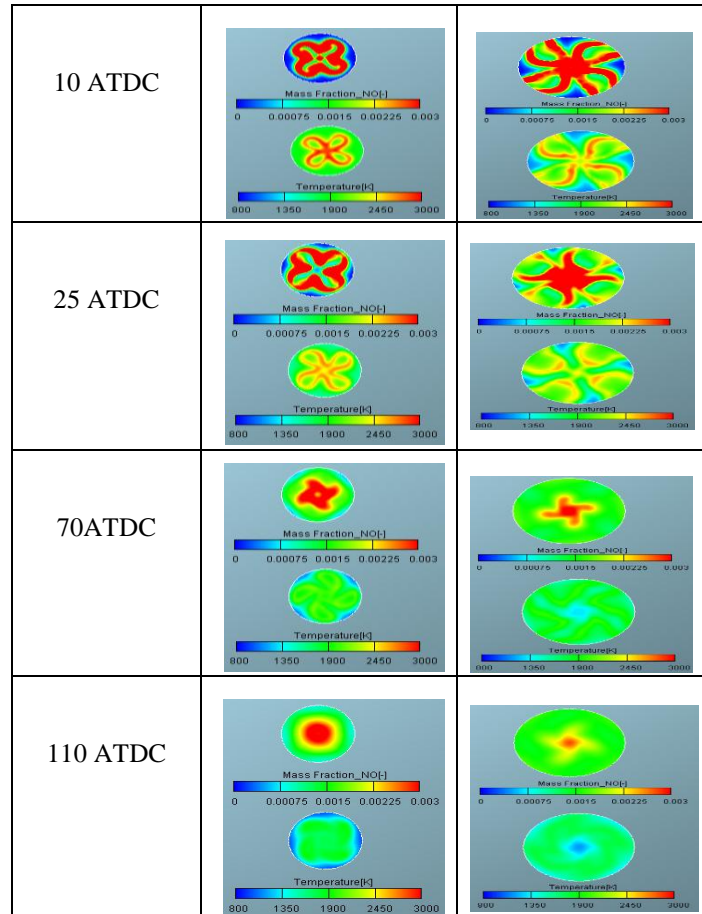|		
10 ATDC		
25 ATDC		
70ATDC		
110 ATDC		

Figure 7. Contour plots for NO and temperature

The NO formation rate varied with the crank angle inside the cylinder, depending on the temperature history of each crank angle. As shown in Figure 7, the temperature gradually decreased as the crank angle increased during the expansion stroke; hence, the rate of NO decomposition rapidly decreased so that, after a crank angle of 110 ATDC, the rates of R6, R7, and R8 (Zel'dovich mechanism) became small. Consequently, the concentration of NO remained almost frozen and did not change during the remainder of the expansion stroke.

Carbon monoxide (CO) emissions:

The variation of carbon monoxide emissions with load is shown in Figure 8. The CO level with hydrogen/diesel (4.83 % H2 by volume) operation was 0.05 % by volume, which was lower than that of baseline diesel 0.16 % by volume at full load.

The CO level gradually decreased with increase in the hydrogen level. The CO level is reduced by 30 %, 40 % and 80 % with 4.8 % H2, 6 % H2 and 11 % H2 by volume respectively as shown in Figure. The CO emission decrease with increasing hydrogen level because of the reason that hydrogen does not contain any carbon in its structure and also because the addition of hydrogen led to reduction in the injected amount of diesel fuel that resulted in CO formation.
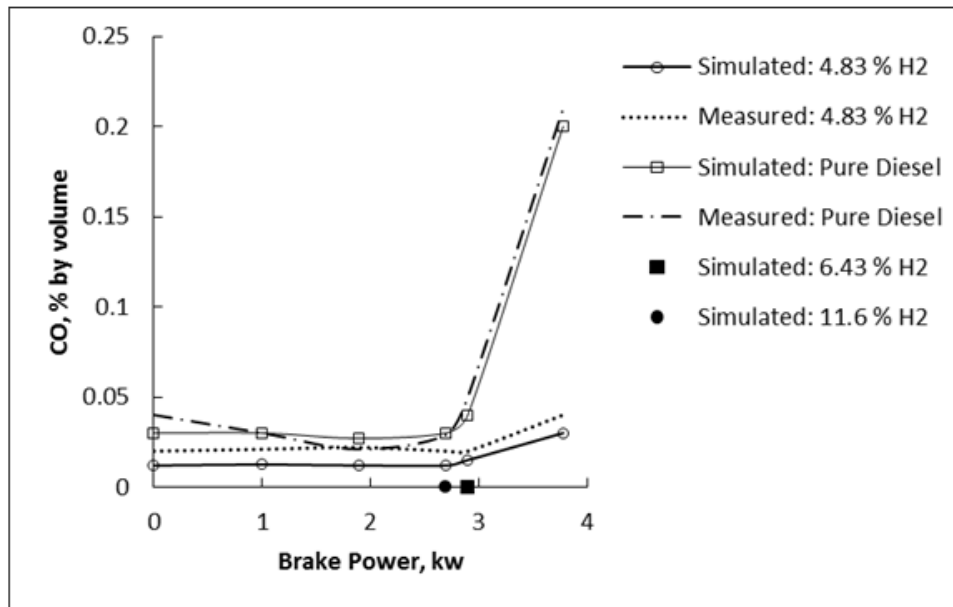
Figure 8. Variation of carbon monoxide with brake power.

Carbon dioxide (CO2) emissions:

The CO2 emissions are lower compared to that of baseline diesel, the minimum being 7.9% by volume at full load at the flow rate of hydrogen as 4.8 % by volume as depicted in Figure 9.The CO2 emission in hydrogen is lowered because of better combustion of hydrogen fuel and also due to the absence of carbon atom in hydrogen flame .

The CO2 value is found to be 8 % by volume with 4.8 H2 % by volume. Further increase in hydrogen flow rate 6.43 % H2 and 11.6 % H2 reduces the CO2 value to 6.6 and 1.06 by volume respectively as shown in Figure. This is because as H2 is added to the intake manifold, the amount of diesel fuel injected is reduced.
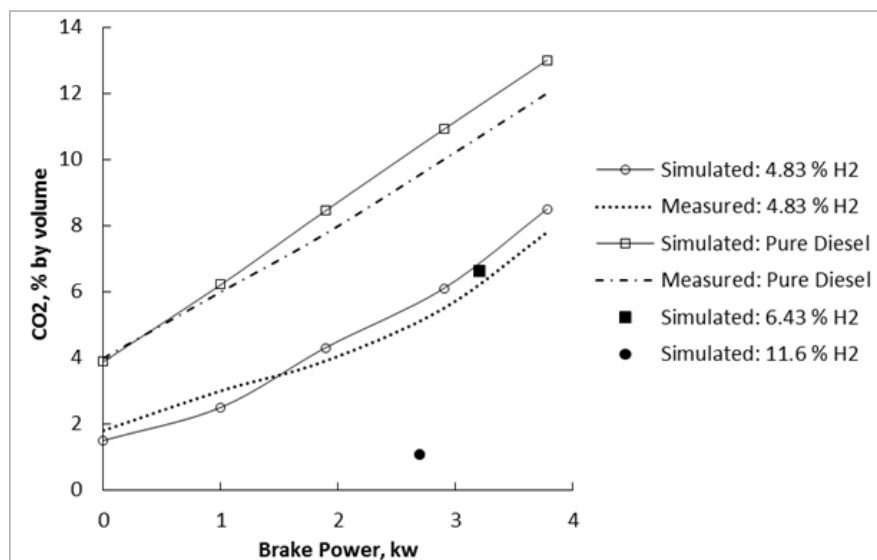

Figure 9. Variation of carbon dioxide with brake power

Figure 10 illustrates an iso-counter of CO and CO_2 at full load for hydrogen-diesel mixture (4.8 % H_2 by volume) and pure diesel, where more CO was observed around the burnt region of fuel. After that, the CO formation region was extended in the cylinders; then, most of the CO formed began to decrease with an increase in the crank angle. due to the conversion of CO to CO_2. This is because the key reaction pathway for CO oxidation is CO + OH = CO_2 + H, (See R26 in Appendix 1), and it was activated by the increased combustion temperature.
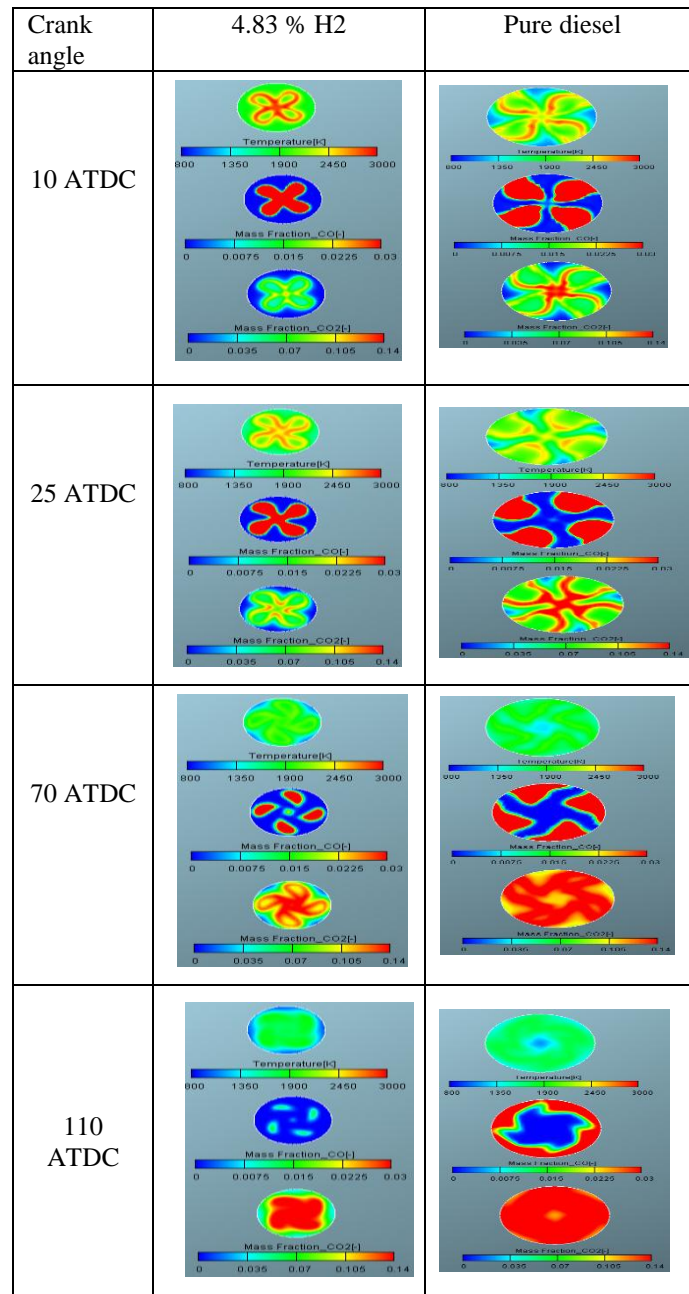
Crank angle	4.83 % H2	Pure diesel
10 ATDC		
25 ATDC		
70 ATDC		
110 ATDC		

Figure 10. Contour plots for CO2, CO, and temperature.

III. CONCLUSIONS

The following conclusions can be drawn from the present research:

➤ The multi-fuel mechanism successfully predicted NO_x, CO and CO_2 emissions in the simulated engineover the four engine loads tested.

➤ The unwanted emissions were reduced drastically with increase hydrogen.

➤ NO_x formation was higher with 37.5% hydrogen level, butbeyond this level, it decreased due to lean burn operation.

➤ The combustion duration became shorter while the ignition delay became longer with increasing the hydrogen level.

➤ The present model successfully demonstrated the capability of describing multi-fuel combustion operations.

ACKNOWLEDGMENTS:

REFERENCES:

[1]. Verhelst, S., and Wallner, T., "Hydrogen-fueled Internal Combustion Engines," Prog. Energ. Combust. 35: 490-527, 2009.
[2]. Subramanian, V., Mallikarjuna, J., and Ramesh, A., "Performance, Emission and Combustion Characteristics of a Hydrogen Fueled SI engine - An Experimental Study," SAE Technical Paper 2005-26-349, 2005, doi:10.4271/2005-26-349.
[3]. Das, L.M., "Hydrogen Engine: Research and Development (R&D) Programmes in Indian Institute of Technology (IIT), Delhi," Int. J. Hydrogen Energ. 27:953-65, 2002.
[4]. Homan, H.S., Reynolds R.K., De Boer, P.C.T., and McLean, W.J., "Hydrogen-fueled Diesel Engine without Timed Ignition," Int. J. Hydrogen Energ. 4:315-325, 1979.
[5]. Naber, J.D., and Siebers, D.L., "Hydrogen Combustion under Diesel Engine Conditions," Int. J. Hydrogen Energ. 23(5):363-371, 1998.
[6]. Welch, A. and Wallace, J., "Performance Characteristics of a Hydrogen-Fueled Diesel Engine with Ignition Assist," SAE Technical Paper 902070, 1990, doi:10.4271/902070.
[7]. Saravanan, N., and Nagarajan, G., "Performance and Emission Study in Manifold Hydrogen Injection with Diesel as an Ignition Source for Different Start of Injection," Renew. Energ. 34:328-334, 2009.
[8]. Priesching, P., and Wanker, R., "Detailed and Reduced Chemistry CFD Modeling of Premixed Charge Compression Ignition Engine Combustion," presented at International Multidimensional Engine Modeling User's Group Meeting, 2003.
[9]. Kong, S., Marriott, C., Reitz, R., and Christensen, M., "Modeling and Experiments of HCCI Engine Combustion Using Detailed Chemical Kinetics with Multidimensional CFD," SAE Technical Paper 2001-01-1026, 2001, doi:10.4271/2001-01-1026.
[10]. Patel, A., Kong, S., and Reitz, R., "Development and Validation of a Reduced Reaction Mechanism for HCCI Engine Simulations," SAE Technical Paper 2004-01-0558, 2004, doi:10.4271/2004-01-0558.
[11]. https://github.com/OpenCFD/OpenFOAM1.7.x/blob/master/tutorials/combustion/dieselFoam/aachenBomb/chemkin/chem.inp_15.